

Supporting information
IR spectra

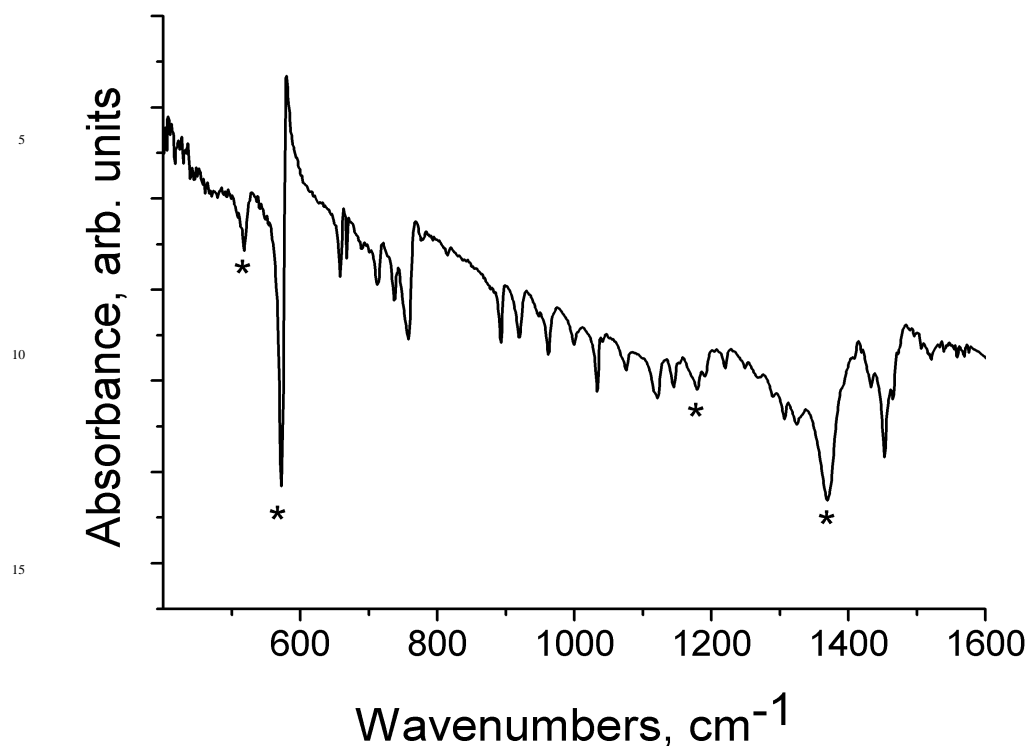
Table S1. IR spectra of **1-4**.

Components	1	2	3	4
Cation ⁺	713w	470w	716w	500s
	758w	495w	747w	533s
	893w	600w	818w	544m
	920w	686w	940m	691s
	962w	751m*	1100s	723s
	1000w	781m	1133s	791w
	1075w	856w	1259w	998w
	1144w	875w	1299m	1115s
	1191w	911w	1355s	1157w
	1220w	953m	1444m	1177w
	1290w	1060m	1455m	1250s
	1306w	1129s	1464m	1271w
	1324w	1162w		1291w
	1453s*	1217m		1306w
	1464m	1255s		1324w
		1281w		1435s
		1328w		1482w
		1357m		1573w
		1451s*		1586w
		1506s		
	1596m			
C ₆₀ ²⁻	518w	527w	527w	525w
	572s	574m	574s	574s
	1180w	-	1181w	1184w
	1370s	1374m	1373s	1373m
Solvents	C ₆ H ₄ Cl ₂	C ₆ H ₄ Cl ₂		C ₆ H ₄ Cl ₂
	658w	658w		660m
	738w	740m		742m
	1033m	1033w		1033w
	1122m	-		-
	1453s*	1451s*		1455w
		C ₆ H ₅ CN		
		549w		
		751m*		
		2235w		

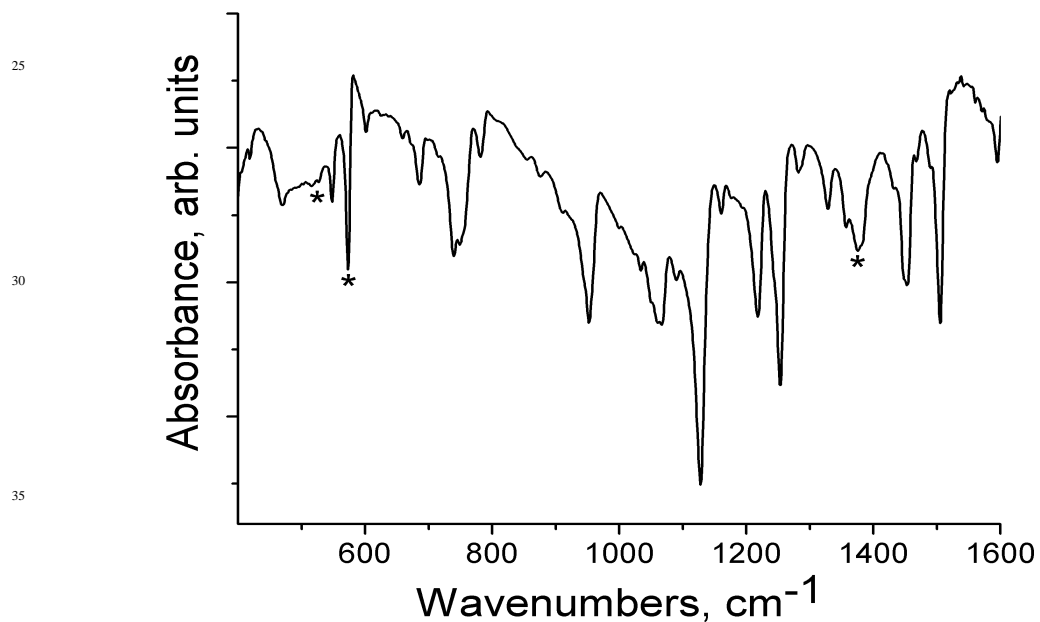
5

10

15



20 **Fig. 1S.** IR spectrum of **1** in KBr pellet measured in anaerobic conditions. The bands of C_{60}^{2-} are marked by stars.



40 **Fig. 2S.** IR spectrum of **2** in KBr pellet measured in anaerobic conditions. The bands of C_{60}^{2-} are marked by stars.

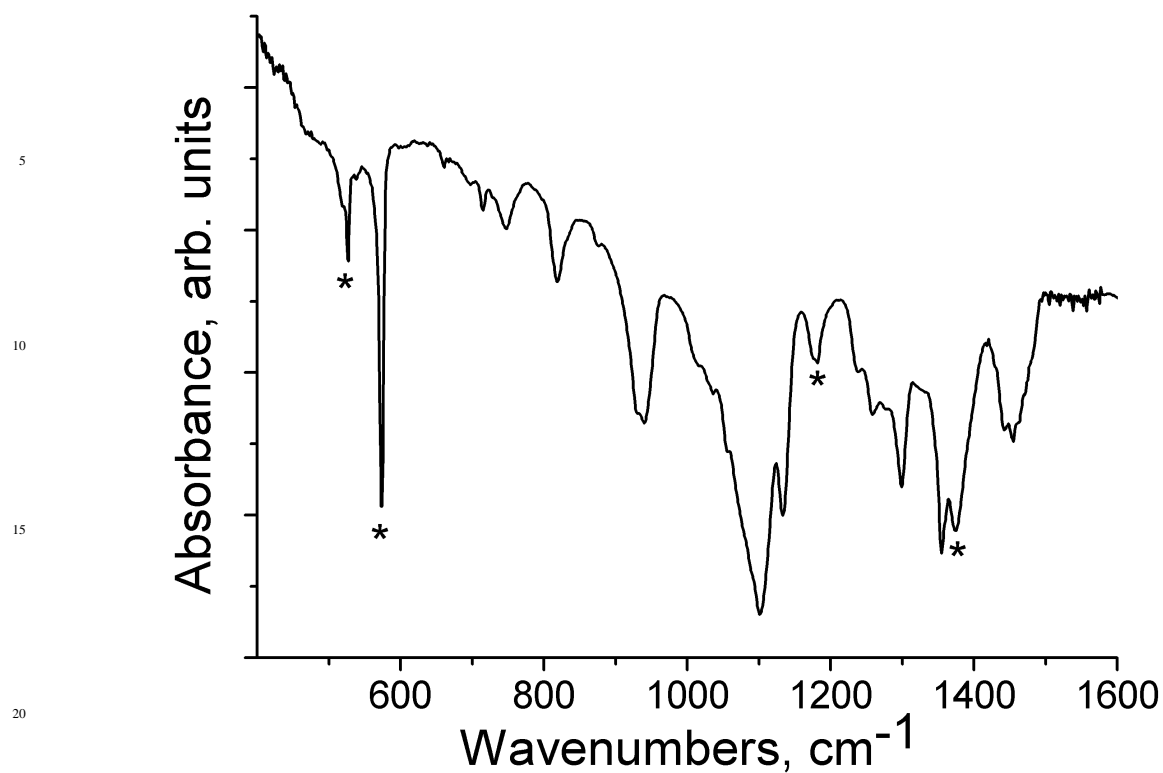


Fig. 3S. IR spectrum of **3** in KBr pellet measured in anaerobic conditions. The bands of C₆₀²⁻ are marked by stars.

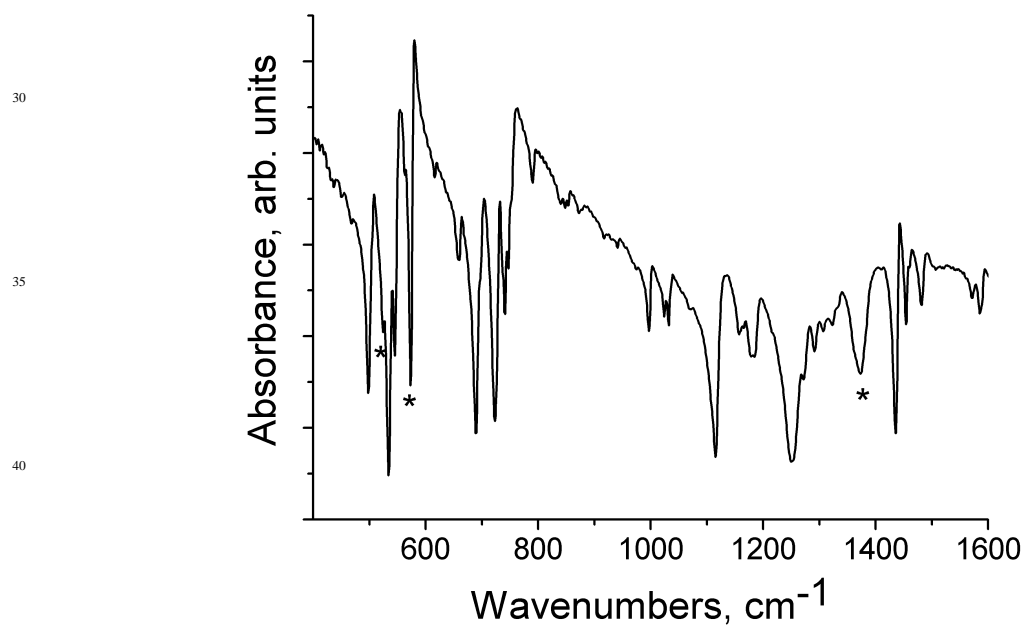


Fig. 4S. IR spectrum of **4** in KBr pellet measured in anaerobic conditions. The bands of C₆₀²⁻ are marked by stars.

UV-vis-NIR spectra.

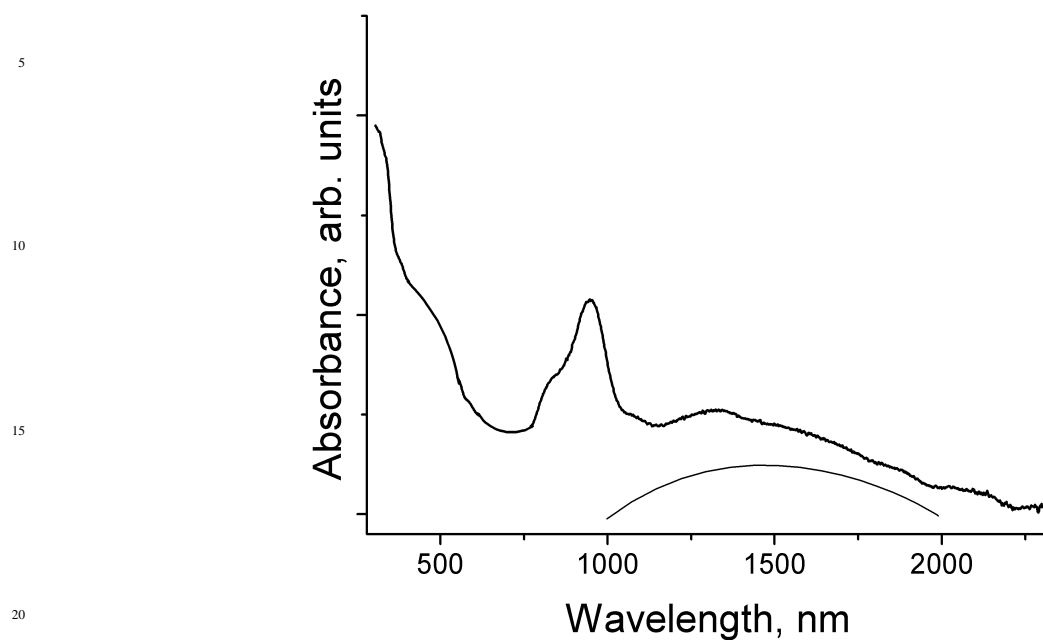


Fig. 5S. Spectrum of **1** in the UV-visible and NIR ranges in KBr pellet measured in anaerobic conditions.

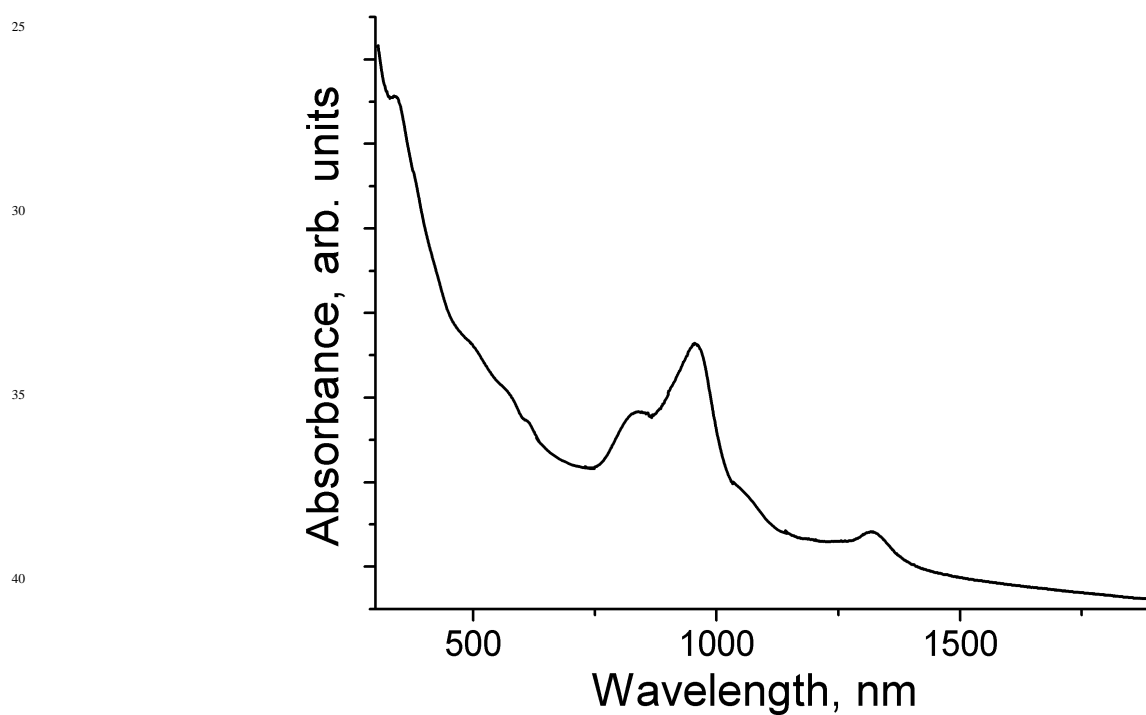


Fig. 6S. Spectrum of **2** in the UV-visible and NIR ranges in KBr pellet measured in anaerobic conditions.

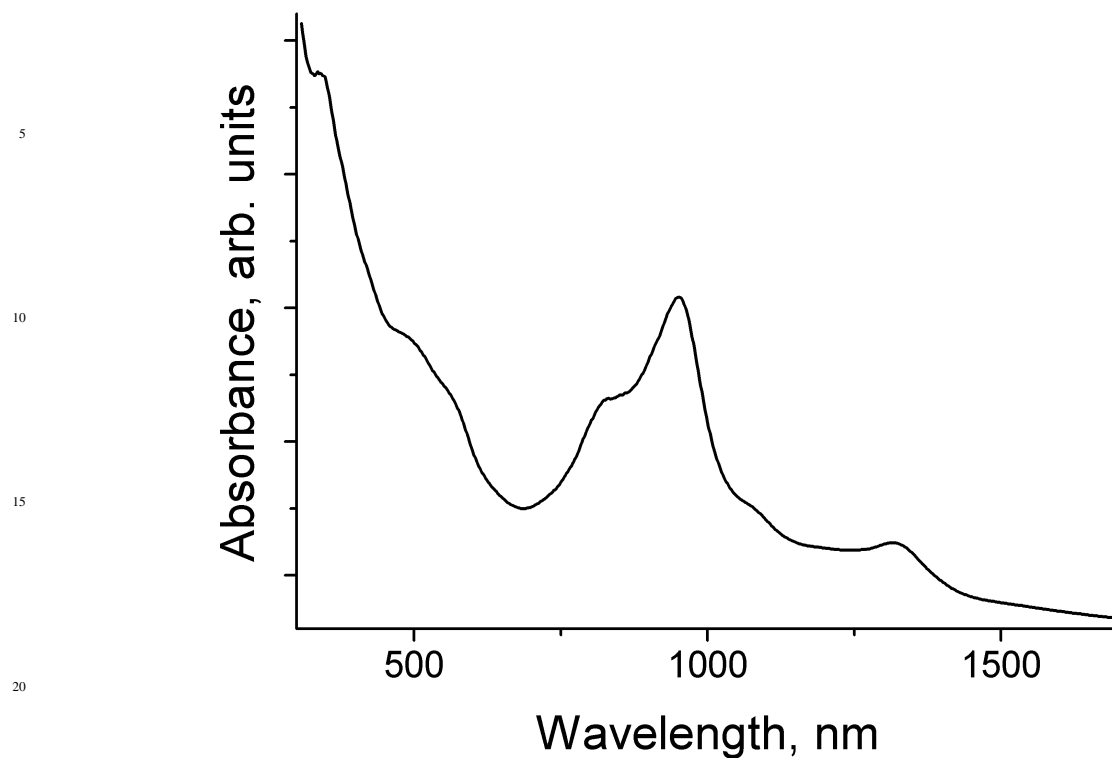


Fig. 7S. Spectrum of **3** in the UV-visible and NIR ranges in KBr pellet measured in anaerobic conditions.

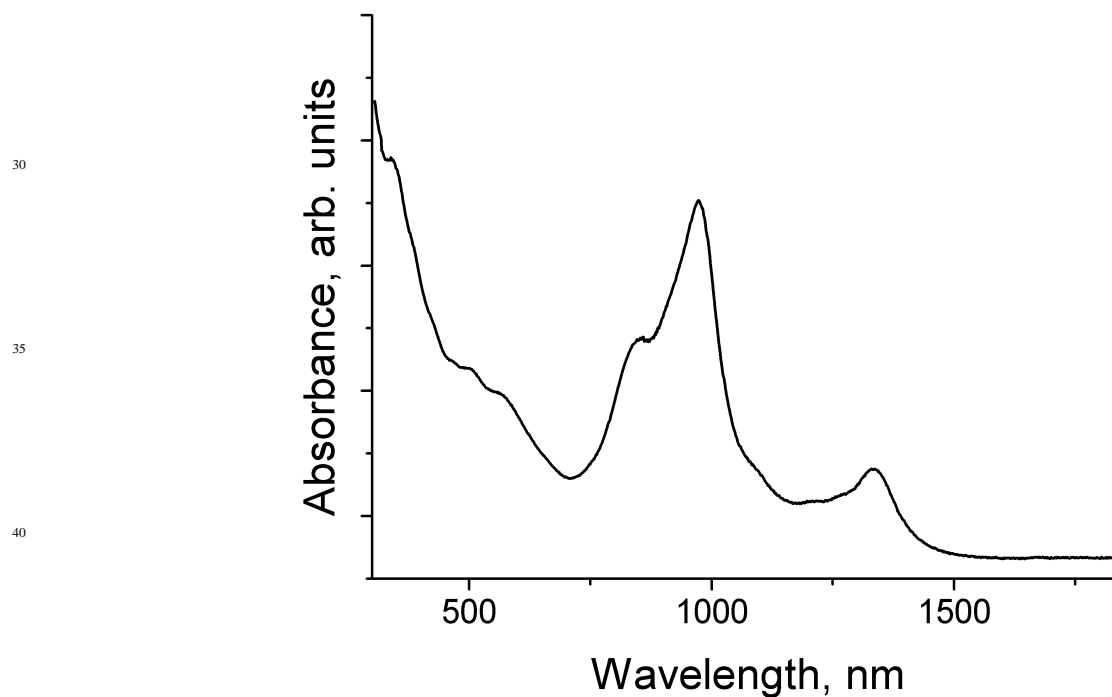


Fig. 8S. Spectrum of **4** in the UV-visible and NIR ranges in KBr pellet measured in anaerobic conditions.

EPR spectra.

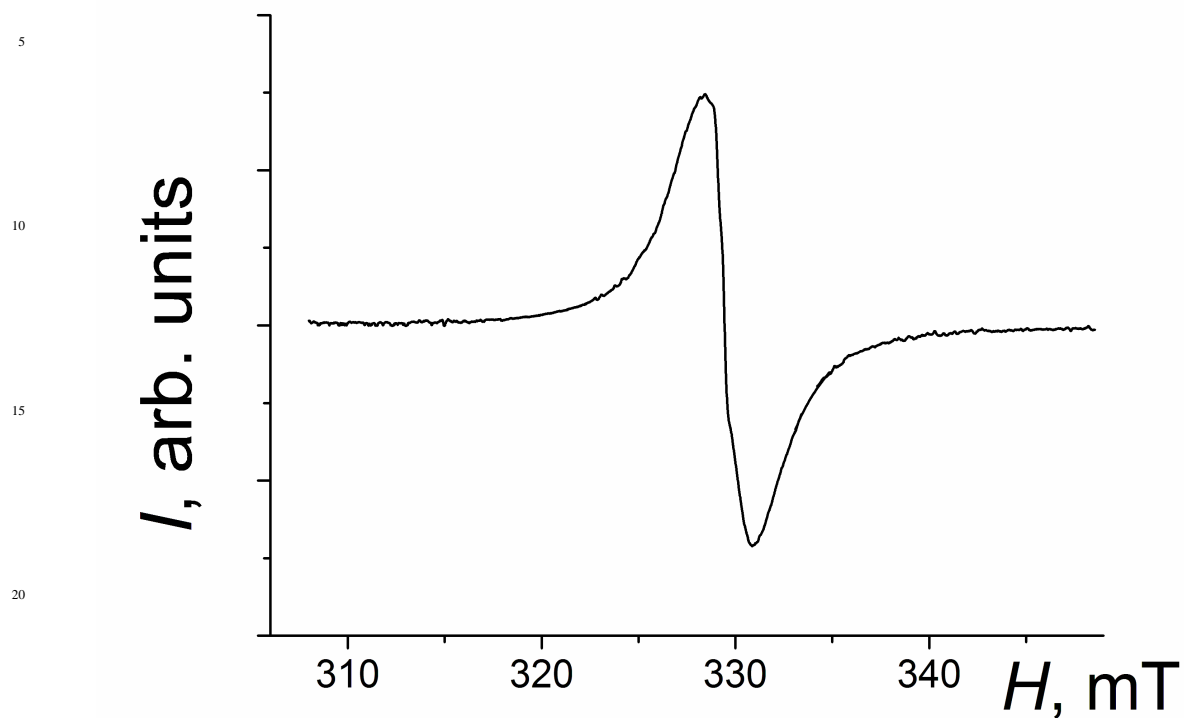


Fig. 9S. EPR spectrum of polycrystalline **1** at room temperature.

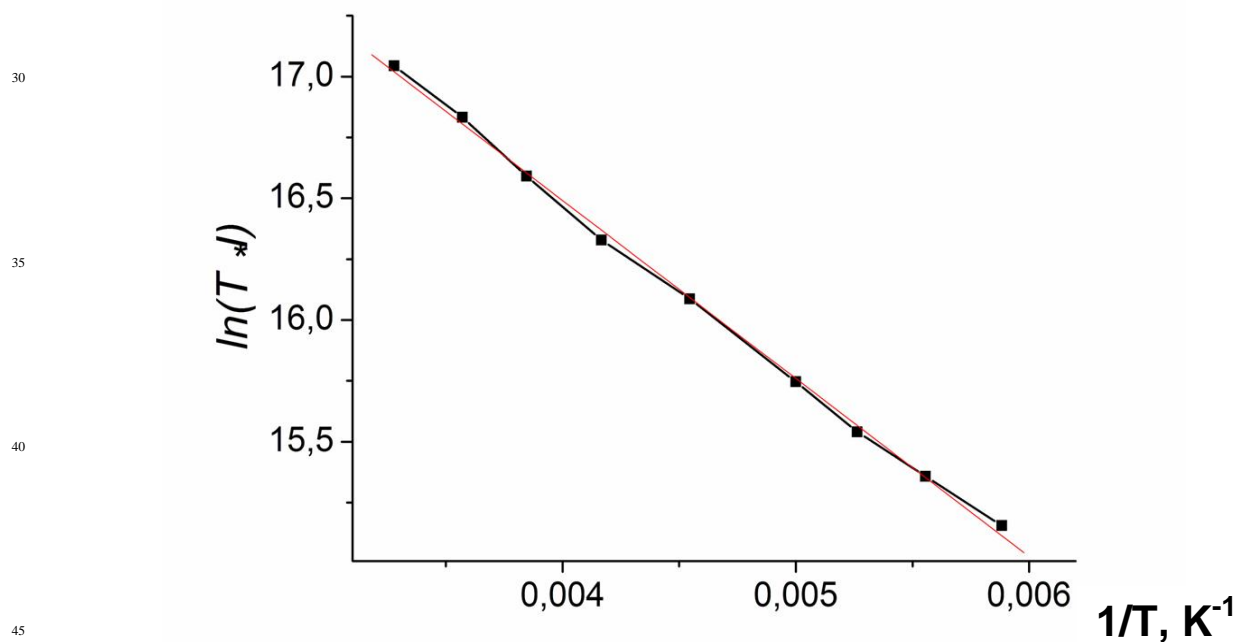


Fig. 10S. Linear dependence of $\ln(T \cdot I)$ versus reverse temperature for polycrystalline **1** in the 170-305 K range.

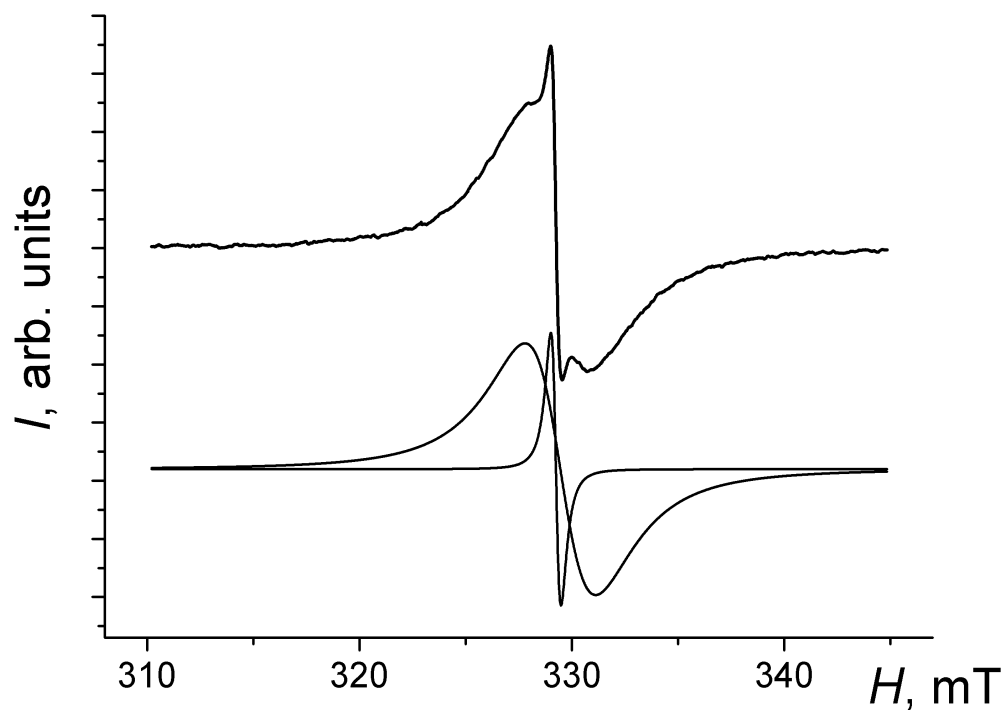


Fig. 11S. EPR spectrum of polycrystalline **2** at room temperature. Below is shown the fitting of the signal by two Lorentzian lines (broad and narrow lines).

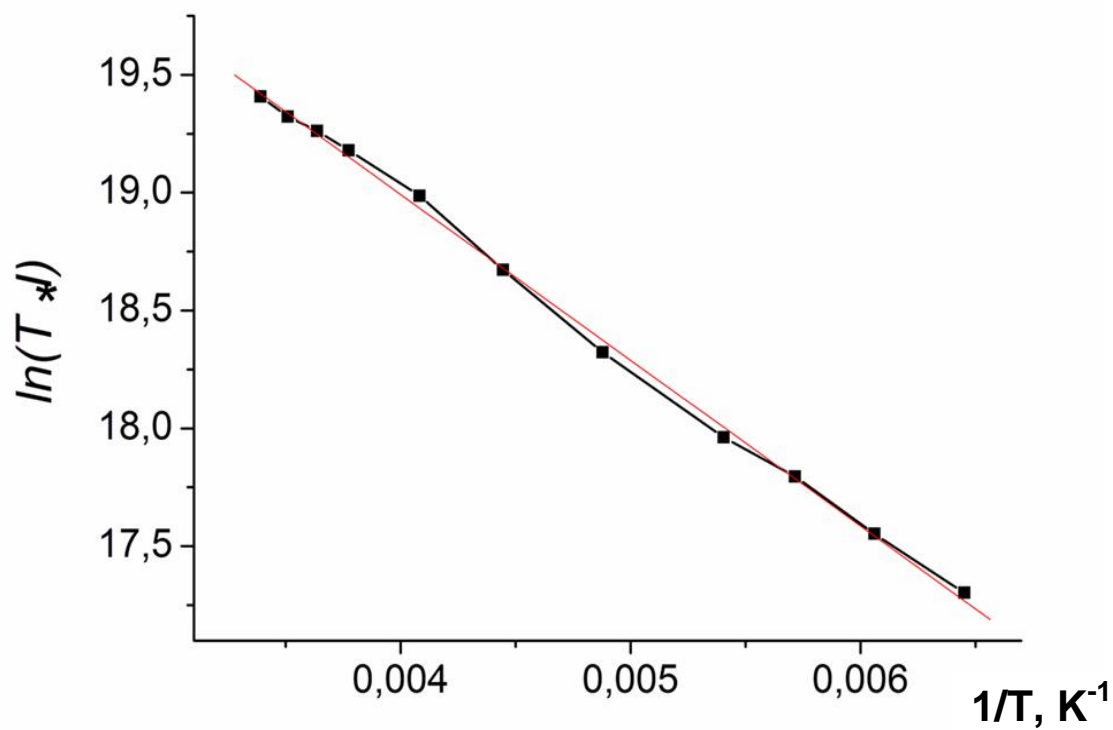


Fig. 12S. Linear dependence of $\ln(T \cdot I)$ versus reverse temperature for polycrystalline **2** in the 155-295 K range.

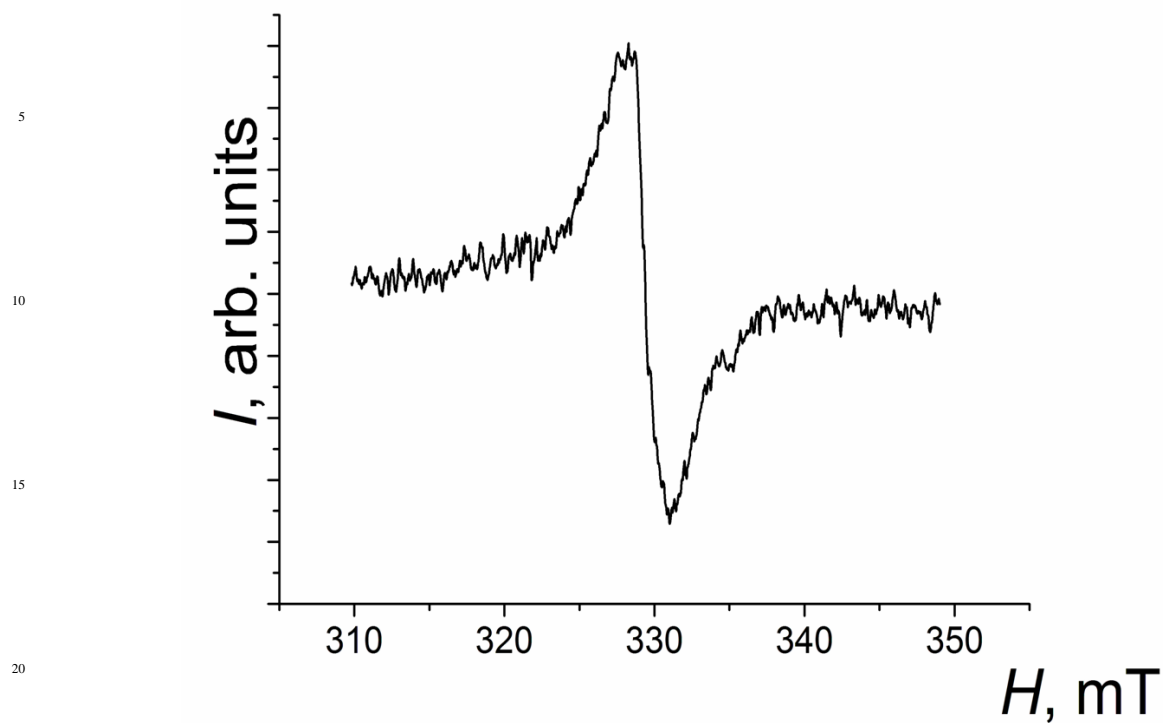


Fig. 13S. EPR spectrum of single crystal of **3** at room temperature.

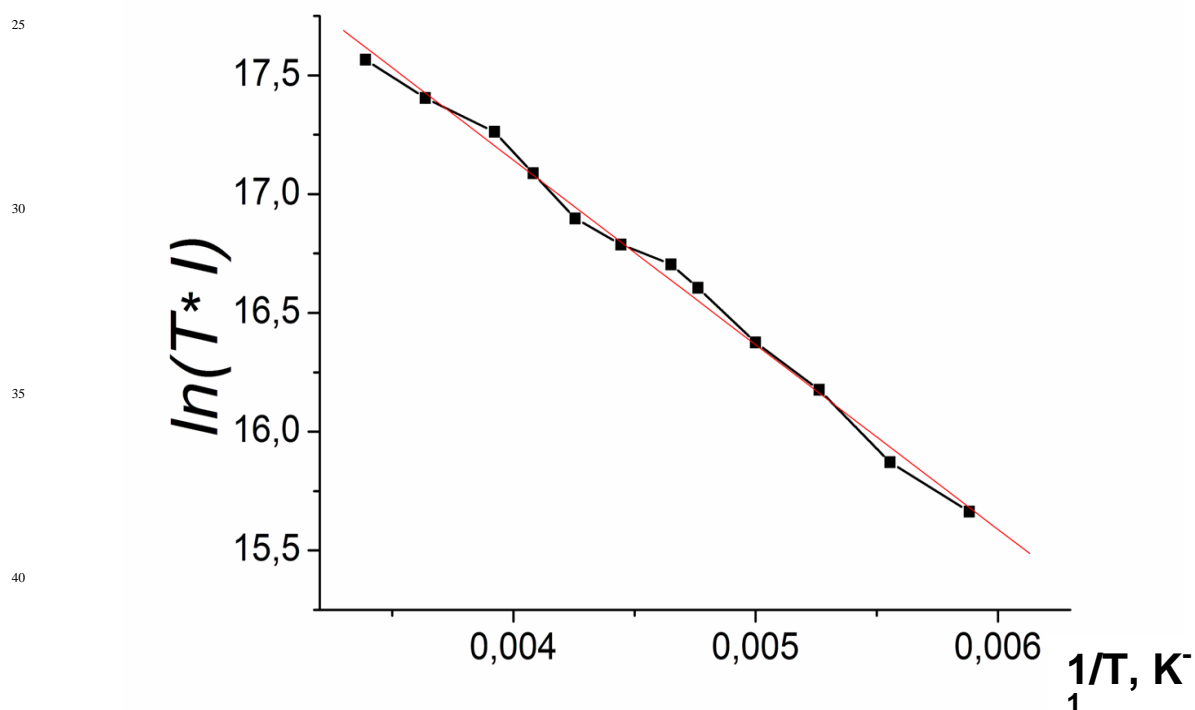


Fig. 14S. Linear dependence of $\ln(T \cdot I)$ versus reverse temperature for single crystal of **3** in the 170-295 K range.

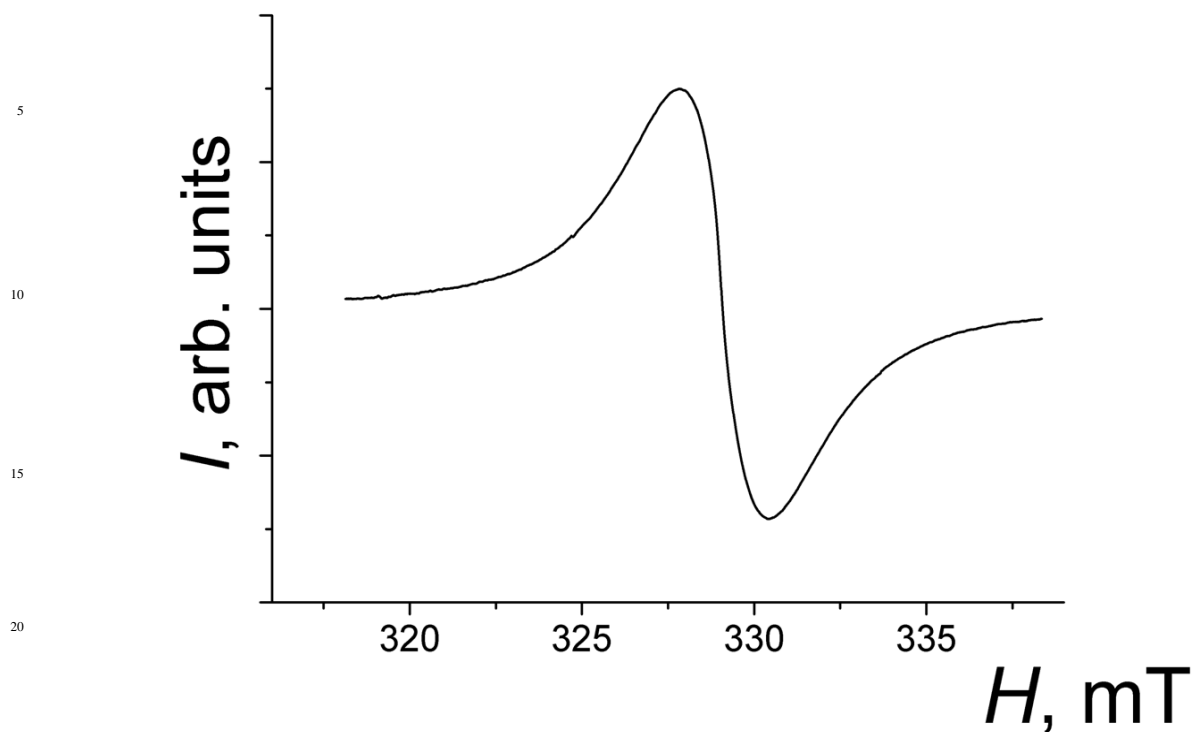


Fig. 15S. EPR spectrum of polycrystalline **4** at room temperature.

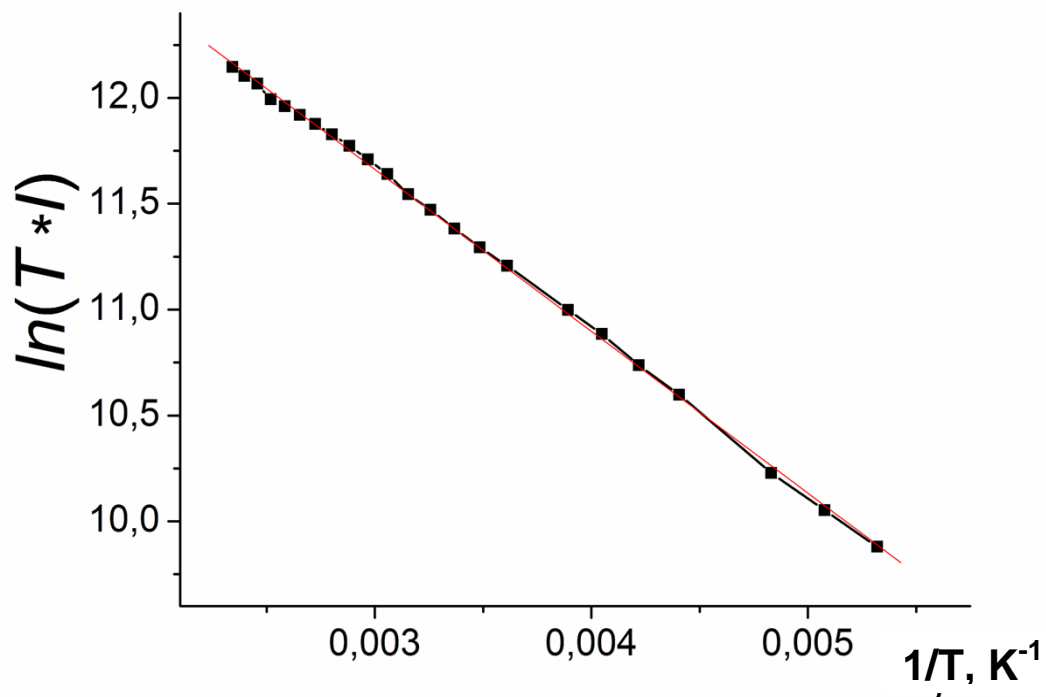


Fig. 16S. Linear dependence of $\ln(T*I)$ versus reverse temperature for polycrystalline **4** in the 190-427 K range.